

<https://doi.org/10.1038/s43247-025-02130-6>

# Freshwater inflows to closed basins of the Andean plateau in Chile, Argentina, and Bolivia

Check for updates

Alexander B. Kirshen<sup>1</sup> ✉, Brendan J. Moran<sup>1</sup>, Lee Ann Munk<sup>2</sup>, Aeon A. Russo<sup>3</sup>, Sarah V. McKnight<sup>4</sup>, Jordan Jenckes<sup>5</sup>, Daniel B. Corkran<sup>1</sup>, Magdalen Bresee<sup>1</sup> & David F. Boutt<sup>1</sup>

More than half the world's lithium resources are found in brine aquifers in Chile, Argentina, and Bolivia. Lithium brine processing requires freshwater, so as lithium exploration increases, accurate estimates of freshwater availability are critical for water management decisions in this region with limited water resources. Here we calculate modern freshwater inflows, such as groundwater recharge and streamflow, for 28 active or prospective lithium-producing basins. We use regional water budget assessments, field streamflow measurements, and global climate and groundwater recharge datasets. Using the freshwater inflow estimates, we calculate water scarcity using the Available Water Remaining methodology. Among all 28 basins, freshwater inflows range from 2 to 33 mm year<sup>-1</sup>. Our results reveal that commonly used global hydrologic models overestimate streamflow and freshwater availability substantially, leading to inaccurate water scarcity classifications.

The renewable energy transition is one of the most important challenges human civilization faces<sup>1</sup>. As green technology continues to advance, batteries for electronic devices, electric cars, and electrical grids are critical<sup>2</sup>. Lithium is a key component in modern batteries, and demand for this critical mineral is projected to increase by as much as 40 times over the coming decades<sup>3,4</sup>. Fifty-three percent of the world's resources of lithium are found in highly saline aquifers (or brines) where evaporation has exceeded precipitation for millions of years, creating elevated concentrations of solutes including lithium<sup>5–9</sup>. These deposits form in closed (or endorheic) basins and are preferentially located in a region of South America referred to as the Lithium Triangle<sup>10,11</sup>.

Although lithium is extracted from brines, freshwater is a key component of lithium production processes<sup>4,12</sup>. After the brine is pumped from wells, it must be processed to produce lithium carbonate or lithium hydroxide (a lithium product for batteries). The two general processing technologies that currently exist on the production scale are evaporative concentration and direct lithium extraction (DLE), which consume variable amounts of freshwater per tonne of lithium carbonate (see Supplementary Notes). The majority of production-scale operations use evaporative concentration, but implementation of DLE is increasing among advanced-stage projects<sup>4,13</sup>. Based on a compilation of freshwater consumption data from scientific articles and reports for various DLE

technologies, 33% consumed less, 11% consumed similar, 25% consumed more, and 31% consumed over 10 times more freshwater than evaporative concentration<sup>4</sup>.

A major challenge with lithium mining in the Lithium Triangle is the lack of modern freshwater inflows from precipitation to sustain water resources for indigenous communities, unique flora and fauna, and mining operations<sup>14,15</sup>. The Lithium Triangle is in the Andean plateau (or Dry Andes) of South America at the intersection of Bolivia, Argentina, and Chile. Elevations are high and variable (2300–6800 m above sea level) with large spatial climate variability. This region is semi-arid to hyper-arid with mean annual precipitation ranging from ~20 mm in the west to ~250 mm in the east<sup>16,17</sup>. Precipitation is event-driven with little to none in the winter and larger events in the summer. Human populations are generally small, but many communities rely on fresh groundwater and surface water resources<sup>14</sup>. Watershed-scale freshwater availability and water scarcity are often assessed with global hydrologic models<sup>1,18–21</sup>. Global hydrologic models provide informative water demand, groundwater, and river discharge data<sup>22–25</sup>. However, in arid regions, traditional hydrologic models often overestimate river discharge<sup>25–27</sup>. While some global models are calibrated to long-term average streamflow<sup>28</sup>, reliable calibration targets on the Andean plateau are highly limited or non-existent.

<sup>1</sup>Department of Earth, Geographic, and Climate Sciences, University of Massachusetts Amherst, Amherst, MA, USA. <sup>2</sup>Geophysical Institute, University of Alaska Fairbanks, Fairbanks, AK, USA. <sup>3</sup>Department of Geological Sciences, University of Alaska Anchorage, Anchorage, AK, USA. <sup>4</sup>Department of Geology and Environmental Geosciences, University of Dayton, Dayton, OH, USA. <sup>5</sup>Department of Computer Science and Engineering, University of Alaska Anchorage, Anchorage, AK, USA. ✉e-mail: [alexander\\_kirshen@mines.edu](mailto:alexander_kirshen@mines.edu)

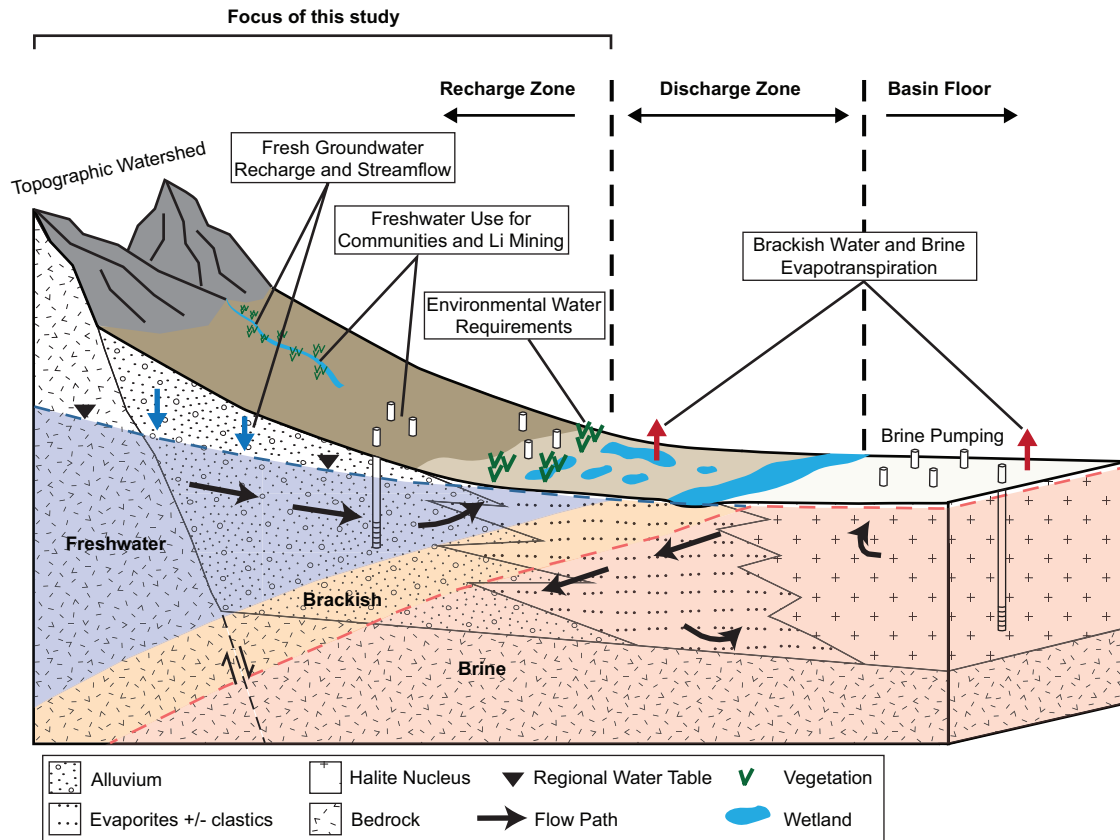


**Fig. 1 | Conceptual block diagram highlighting the generalized hydrogeology of the closed basins in this study.** The basins can be divided into three zones: the recharge zone, the discharge zone, and the basin floor. The diagram includes modern freshwater sources (fresh groundwater recharge and streamflow) and freshwater demand (freshwater use for communities and lithium mining and environmental water requirements). Groundwater recharge is shown by dark blue arrows, regional

groundwater flow paths as black arrows, and vegetation as green “V” shapes. Water salinity is represented by shaded areas beneath the water table: freshwater (blue), brackish water (yellow), and brine (red). The major outflow from these basins is evapotranspiration, primarily from brackish water and brine (red arrows). The focus of this study is the freshwater processes occurring in the recharge zone. This figure is vertically exaggerated.

The hydrogeology of these closed-basin systems is complex (Fig. 1). Precipitation in the recharge zone (as both snow and rain) is the only modern freshwater input into these basins<sup>29,30</sup>. Freshwater flows from the topographic watershed boundary toward the lower-elevation basin floor, where it contacts brine. The interface between the freshwater and the brine forms a saline wedge due to the density differences between the two waters. When freshwater reaches the discharge zone, it discharges above the brine to the land surface forming brackish and brine lagoons and wetlands, where it ultimately evaporates or transpires<sup>31,32</sup> (Fig. 1). The wetland areas have large seasonal fluctuations and are sustained by both modern precipitation and groundwater storage<sup>33–35</sup>. These wetlands are home to diverse and sensitive ecosystems ranging from microbial lagoon communities to larger fauna<sup>36,37</sup>. Both perennial and intermittent freshwater streams exist in the higher-elevation mountains near the topographic watershed boundaries, which are largely sourced from groundwater storage<sup>38,39</sup>. These streams can extend to the brine aquifer or disappear before reaching the basin floor due to evapotranspiration or infiltration into groundwater<sup>40</sup>. Streamflow must be considered when addressing freshwater availability in these systems because it is crucial for sustaining diverse wetlands and ecosystems and is sometimes utilized as a freshwater resource for communities and mining<sup>36</sup>. Another important hydrogeologic factor to consider is hydrostratigraphy, which contributes to the behavior of streams, wetlands, and lagoons, and plays a role in how these systems respond to freshwater and brine withdrawals<sup>32,41,42</sup>. The generalized lithology of these basins contains three units: upgradient alluvium, marginal evaporites, and a halite nucleus<sup>11</sup> (Fig. 1). Freshwater use from surface water and groundwater

(well pumping) occurs upgradient of the discharge zone, reducing freshwater flow to wetlands<sup>42,43</sup>. Brine pumping for lithium mining usually occurs downgradient of the discharge zone in the brine aquifer and may reduce discharge to wetlands, although the effects of brine pumping on wetland discharge are buffered by hydrogeologic processes<sup>42,44</sup>. The processes occurring in the recharge zone are the focus of this study (Fig. 1).

A growing body of research is investigating the influence of lithium brine mining activities on local communities, ecosystems, and water scarcity<sup>4,14,34,45–56</sup>. With growing concerns over environmental and societal impacts, battery manufacturers and society will need to further consider the sustainability of their lithium sources. Accurate estimates of freshwater availability are imperative<sup>57</sup>, as they are often a key input into lithium-related life cycle assessments (LCAs) and are used for water management decisions<sup>47,48,58–60</sup>. This will become ever more important as the impacts of global climate change in this region become more pronounced. These impacts include rising temperatures, increasing length and severity of droughts, the frequency and intensity of anomalous precipitation events, and the potential for declines in rock glaciers<sup>14,34,61</sup>.

The study presented here addresses the following questions: (1) how much freshwater naturally recharges aquifers or flows as freshwater streams within these closed basins, and (2) how do revised freshwater inflows change the current understanding of freshwater in the Lithium Triangle in the context of water stress and availability. To answer these questions, we developed the Lithium Closed Basin Water Availability (LiCBWA) model to assess basin-scale water availability for 12 active or near-production and 16 prospective lithium-producing basins.

## Results and discussion

### Precipitation assessment

To identify the precipitation product with the most reliable long-term average representation of the region's precipitation, we compared mean annual precipitation from 13 global datasets with observations from 26 meteorological stations. The TerraClimate model produces the most accurate long-term average precipitation for the region, so we use TerraClimate as input into our freshwater availability calculations<sup>62</sup>. Detailed results from this assessment are included in Supplementary Information (Supplementary Figs. 1–3, Supplementary Table 1).

### Basin-scale freshwater availability and demand

The LiCBWA model utilizes terminology and methodology from the Available Water Remaining (AWARE) LCA midpoint indicator. AWARE assesses global water scarcity and quantifies the amount of water remaining in a watershed after demands for humans and ecosystems have been met<sup>18</sup>. The LiCBWA model has three components adopted from AWARE: available freshwater (AW), freshwater demand, and availability minus demand.

The major difference between LiCBWA and AWARE is our method of calculating AW; available water in AWARE is defined as river discharge from the WaterGAP2.2 hydrologic model<sup>18,63</sup>, whereas we define AW as the sum of modern fresh groundwater recharge (GWR) and freshwater streamflow using region-specific calculations. Freshwater demand is the sum of human freshwater consumption (from the WaterGAP model) and environmental water requirements (EWR) (or the freshwater required to sustain ecosystems). The WaterGAP model does not consider freshwater use from lithium mining. Availability minus demand equals AW minus freshwater demand; lower availability minus demand indicates a higher probability of water scarcity within a basin. We calculate baseline availability minus demand, which indicates water scarcity prior to or regardless of water impacts from lithium mining.

AW, freshwater demand, and availability minus demand results are shown in Fig. 2 and Supplementary Table 2. Average precipitation from TerraClimate ranges from 20 to 205 mm year<sup>-1</sup> with coefficients of variation ranging from 0.16 to 0.66 (Supplementary Fig. 4 and Supplementary Table 3). AW generally increases moving east following trends in precipitation and varies between 2 and 33 mm year<sup>-1</sup> (Fig. 2a). Freshwater demand varies between 1 and 15 mm year<sup>-1</sup> with demand increasing to the east (Fig. 2b). Demand is dominated by EWR, contributing on average 95% of total demand. Availability minus demand follows a similar geographic trend to AW, with values ranging from 1 to 18 mm year<sup>-1</sup> (Fig. 2c). The average annual availability minus demand for all 28 basins is 6 mm, a stark contrast to the world average of ~160 mm<sup>18</sup>.

### Comparison with WaterGAP 2.2 and PCR-GLOBWB 2.0

We compare our results with stream discharge outputs from two hydrologic models: WaterGAP 2.2 and PCR-GLOBWB 2.0<sup>63,64</sup>. WaterGAP and PCR-GLOBWB are the input models for widely used water scarcity and availability products like the National Geographic and Utrecht University Water Gap, Aqueduct Water Risk Atlas, World Wildlife Fund Water Risk Filter, and AWARE<sup>18–21</sup>. These hydrologic models are also used to assess current global water security and projected future streamflow in the Sixth Assessment Report from the Intergovernmental Panel on Climate Change<sup>1,65,66</sup>. First, we compare the accuracy of streamflow estimates for all three models with streamflow field measurements. Second, we compare our AW results (fresh GWR plus streamflow) with AW outputs from WaterGAP and PCR-GLOBWB. Third, we calculate a characterization factor (CF) for each basin and identify how AWARE CFs and water scarcity classifications differ for each basin depending on which of the three models are used as input (LiCBWA, WaterGAP, or PCR-GLOBWB). The AWARE CF is calculated based on availability minus demand relative to the world average and describes regional water scarcity with larger values indicating higher water scarcity and less freshwater remaining per area<sup>18</sup>.

Our model (LiCBWA) provides the most accurate streamflow estimates with a mean absolute error of 3 mm year<sup>-1</sup> (26%), while the mean absolute error for WaterGAP and PCR-GLOBWB are 168 mm year<sup>-1</sup> (1322%) and 482 mm year<sup>-1</sup> (3800%), respectively (Fig. 3a). When comparing AW estimates from LiCBWA with WaterGAP and PCR-GLOBWB, WaterGAP is greater than LiCBWA in 61% of basins, while PCR-GLOBWB is greater in 96% of basins. On average, WaterGAP and PCR-GLOBWB estimate AW to be 75 and 219 mm greater than LiCBWA estimates (Fig. 3b). The median AW (excluding outliers) of all 28 basins from LiCBWA is 10 mm year<sup>-1</sup>, while the median AW from WaterGAP and PCR-GLOBWB are 55 and 165 mm year<sup>-1</sup> (Fig. 3c).

The AWARE CF for each basin varies when using inputs from the three models, which changes water scarcity classifications (Fig. 3d). LiCBWA classifies more basins as critical (27) compared to WaterGAP (13) and PCR-GLOBWB (1). Of the basins where we have field streamflow measurements and greater confidence in availability minus demand and CFs (Salar de Atacama, Salar de Pastos Grandes, and Salar del Hombre Muerto), LiCBWA classifies all three as critical, WaterGAP classifies Salar de Atacama as critical, and PCR-GLOBWB classifies all three as uncritical (Fig. 3d). When using measured streamflow for these basins, they are all classified as critically water-scarce.

### Simplified and improved freshwater inflow conceptualization

We provide a water budget conceptualization unique to arid, endorheic basins of the Dry Andes. Global hydrologic models can be complex with multiple water compartments (e.g., canopy, snow, soil, surface water, groundwater) and include meteorological forcings where surface water and groundwater storage are calculated on a cell-by-cell basis<sup>22,28</sup>. Because this region consists of only endorheic basins, we assume that each watershed is a closed hydrologic system where all modern fresh GWR and streamflow is sourced from precipitation and storage within basin boundaries, such that freshwater demand will impact AW only in the corresponding basin. With this assumption, we can simplify the approach by calculating long-term average GWR and streamflow using region-specific understanding and methods. We indirectly model evapotranspiration through our AW approach instead of using actual evapotranspiration products which have large uncertainties<sup>25,67</sup>. We use human water consumption (HWC) data from the WaterGAP model because human freshwater consumption (excluding lithium mining) is difficult to quantify due to limited data and reporting. The Salar de Atacama is the only basin in the study region with detailed basin-wide freshwater allocation and estimated use data published<sup>34</sup>. In the Salar de Atacama, WaterGAP predicts 330 L s<sup>-1</sup> of freshwater use, while the published data estimates ~1200 L s<sup>-1</sup> of freshwater consumption for agriculture, domestic, tourism, and other uses. With improved water use reporting, HWC can be modified to improve the accuracy of this methodology.

Our study improves the current understanding of how much freshwater is naturally available in the Lithium Triangle. Based on measured streamflow data, our AW results (LiCBWA) are more accurate than WaterGAP and PCR-GLOBWB. In general, these two models overestimate streamflow, which is connected to an overestimation of precipitation. In the Salar de Atacama, the input climate model to WaterGAP (Watch Forcing Data applied to ERA-Interim<sup>68</sup>) overestimated precipitation by 20 mm year<sup>-1</sup>, and the modeled input precipitation for PCR-GLOBWB overestimated by 94 mm year<sup>-1</sup>; this is based on the seven meteorological stations within the basin polygon. Corresponding simulated river discharge is within 1 mm year<sup>-1</sup> for WaterGAP and overestimated by 205 mm year<sup>-1</sup> for PCR-GLOBWB. In the Salar del Hombre Muerto, input precipitation is overestimated by a staggering 570 mm year<sup>-1</sup> for WaterGAP and 191 mm year<sup>-1</sup> for PCR-GLOBWB (based on 1 meteorological station within the basin polygon). Corresponding simulated river discharge is overestimated by 270 mm year<sup>-1</sup> for WaterGAP and 970 mm year<sup>-1</sup> for PCR-GLOBWB. The positive correlation between streamflow and precipitation has been previously shown for both models, as well as for other global water models<sup>25</sup>. The other likely source of overestimation is the specific method of



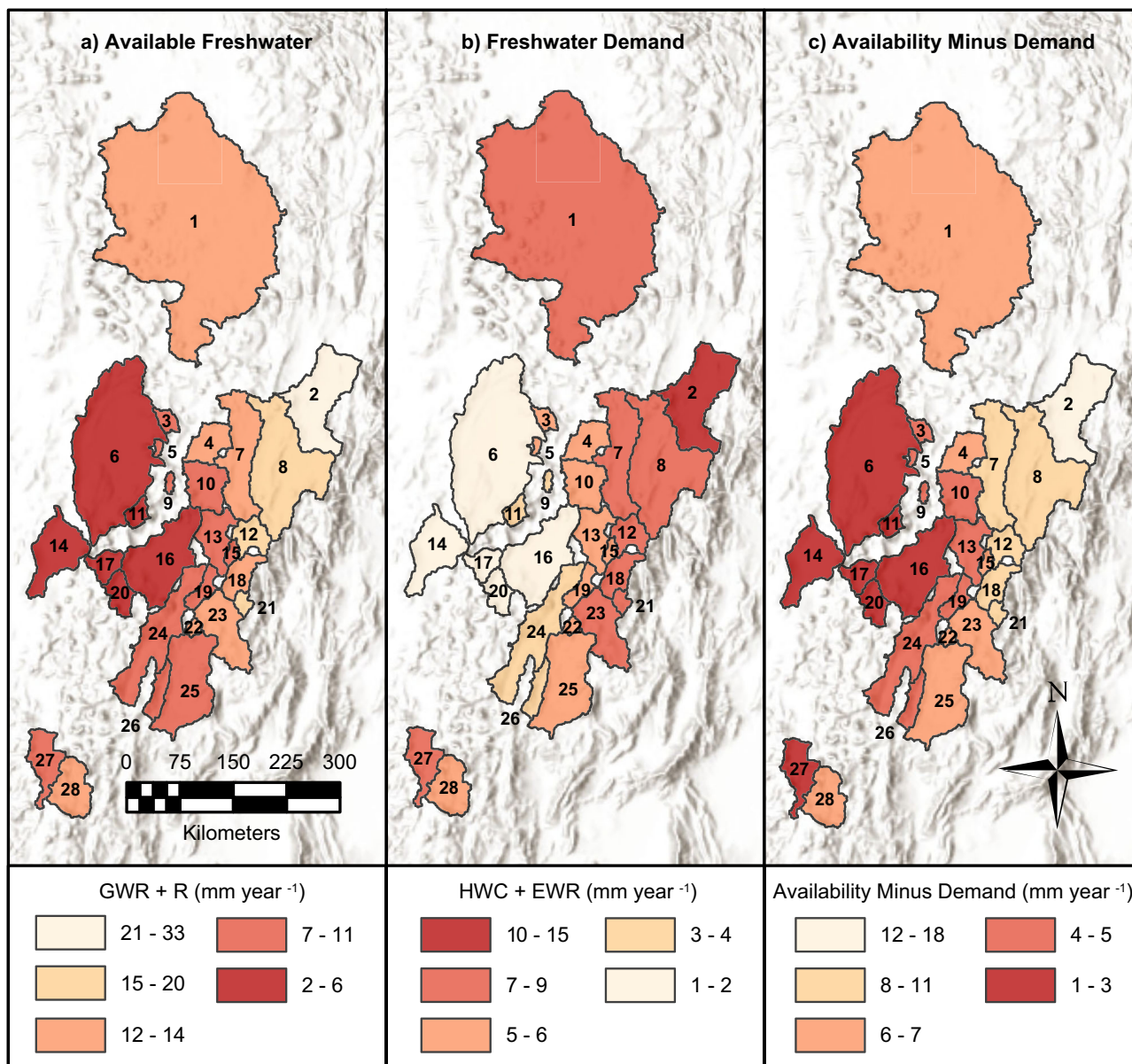


**Fig. 2 | Results of available freshwater, freshwater demand, and availability minus demand calculations.** **a** Average available freshwater calculated as groundwater recharge (GWR) plus streamflow (R) with darker red showing less available freshwater. **b** Freshwater demand calculated as human water consumption from WaterGAP (HWC) plus environmental water requirements (EWR) with darker red

showing more freshwater demand. **c** Average availability minus demand is calculated as available freshwater minus freshwater demand with darker red showing less availability minus demand. The maps include topographic hillshade (image source: ESRI).

simulating streamflow generation. On average 19% of precipitation becomes streamflow (range of 0–43%) in the WaterGAP model, and 101% of precipitation becomes streamflow (range of 9–321%) in PCR-GLOBWB. The upper end of these ranges is unrealistic in endorheic basins, particularly when streamflow is greater than precipitation (>100%)<sup>30,69</sup>. The LiCBWA approach estimates that 12% of precipitation becomes average AW (fresh GWR plus streamflow) within a range of 9–16%.

The work here highlights challenges within existing water scarcity concepts. Freshwater inflows in closed (endorheic) basins in this region are poorly represented by two of the commonly used global hydrologic models, so using water stress indicators based on these models could provide inaccurate results in LCA and water use impact studies. We believe our revised availability minus demand and AWARE CF calculations should be adopted for lithium-related water scarcity assessments. Recent studies highlight the importance of developing a modified AWARE calculation specifically for basins in the Lithium Triangle<sup>59,60</sup>.

Although the LiCBWA model is calibrated based on region-specific data, our method can be extended to other closed basins around the world.

Uncertainty remains in the fresh GWR and fresh streamflow estimates associated with the complex hydrologic dynamics of these basins and the climate and streamflow monitoring network across the study region. Some streamflow and groundwater may be sourced from long flow paths from adjacent basins. In addition, some inflow may be from long recharge pathways and groundwater storage releases that represent wetter climates of the past<sup>33,34</sup>. Accurate streamflow measurements are limited to three basins in the region. Although these three basins represent a relatively large range of elevation, annual precipitation, and area, they may not be representative of all the basins analyzed. While many basins in the study have streamflow or runoff, some of the basins may have limited to no sustained streamflow. For the basins with no sustained streamflow, our calculation that 9–16% of precipitation enters the modern freshwater system (as AW) is reasonable for

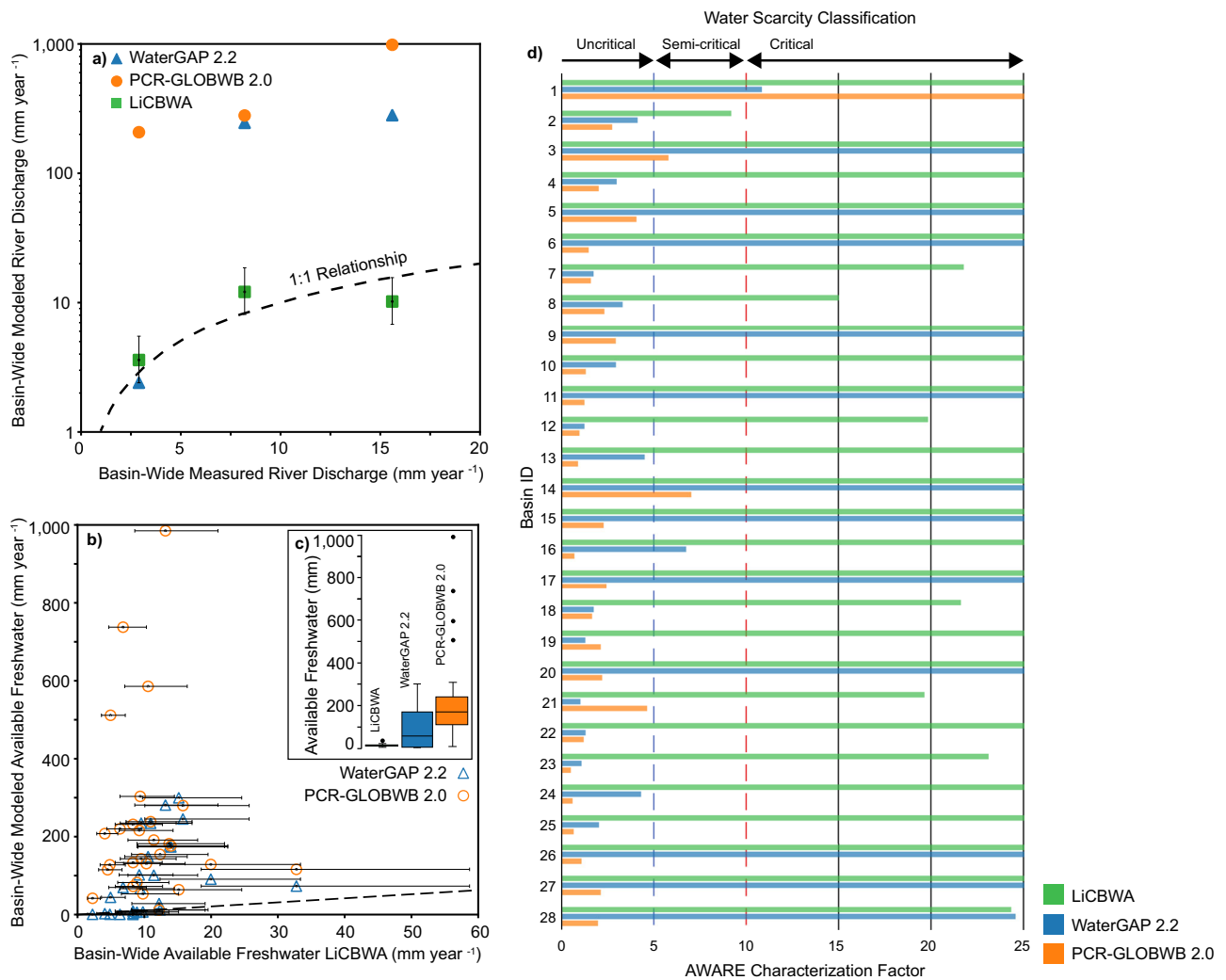


**Fig. 3 | Comparing results from this study with PCR-GLOBWB and WaterGAP.** **a** Basin-wide average modeled river discharge vs. basin-wide river discharge from field measurements (3 total) for WaterGAP (blue triangle), PCR-GLOBWB (orange circle), and this study (LiCBWA, green square). Upper and lower bounds are included for LiCBWA and represent the minimum and maximum streamflow calculations. **b** Basin-wide modeled available water from WaterGAP (blue triangle) and PCR-GLOBWB (orange circle) vs. basin-wide average modeled available freshwater from LiCBWA for all 28 basins. Upper and lower bounds are defined from ranges in

groundwater recharge and streamflow. **c** Box plots of average available freshwater for all three models. The box is bounded by the IQR, and the outliers are greater than  $1.5 \times$  the IQR. **d** Water scarcity classifications based on average availability minus the demand for all 28 basins (labeled on the vertical axis). The bottom axis shows AWARE characterization factors calculated from WaterGAP (blue), PCR-GLOBWB (orange), and LiCBWA (green). The top axis shows water scarcity classifications from Schomberg et al.<sup>48</sup>, with CF cutoffs represented as blue and red dotted lines.

arid basins in this region and does not impact our results<sup>30</sup>. Additionally, the meteorological stations used here have limited coverage in the south of the study region and between 2700 and 3200 m above sea level (Supplementary Figs. 1 and 2).

To continue improving the quantification of freshwater availability, the hydrologic, geochemical, and meteorological monitoring network must be expanded. Measuring monthly streamflow in additional basins will improve our understanding of streamflow generation. Seasonal geochemical water sampling of fresh groundwater, transitional groundwater, streamflow, and lagoons will help define the sources and ages of water to continue improving how we define freshwater availability in the Dry Andes. Installing meteorological stations in active and potential lithium-producing basins with an expanded range of elevations will allow for continued improvement of precipitation products. With further research and an improved understanding of the interactions between the brine and freshwater aquifers, the freshwater and brine systems can be coupled with an integrated available water and demand assessment.

### Implications for water resource management

Lithium mining requires freshwater<sup>4</sup>, therefore it is important to quantify freshwater inflows in this data-sparse region. Freshwater abstraction in these basins has a direct and immediate impact on groundwater-dependent ecosystems. With our improved quantification of freshwater inputs, we find that all but one of the basins in the study is classified as critically water-scarce without incorporating current or future freshwater use from mining. To evaluate the relative impacts of freshwater and brine consumption, we can use insights from a groundwater modeling study that simulated how groundwater discharge to wetlands changes due to freshwater and brine pumping at the Salar de Atacama and the Salar del Hombre Muerto<sup>42</sup>. It has been shown that proportionally, fresh groundwater pumping leads to larger reductions in fresh groundwater discharge to wetlands than brine pumping. However, brine pumping impacts vary depending on the proximity of the abstraction location to the wetland, such that where brine withdrawals occur near or beneath wetlands, localized reductions in groundwater discharge to wetlands can approach those of freshwater withdrawals<sup>42</sup>. Therefore, any quantification of lithium mining impacts on water resources requires basin-

specific knowledge of freshwater and brine abstraction points as well as wetland delineation.

Total water use (brine and freshwater) from lithium production has become a major point of contention over the past decade. Concerns focus on the disruption of available water for society and ecosystems. The risks to wetland ecosystems and groundwater resources have been appropriately highlighted over the last several years<sup>14,54</sup>. However, when determining impacts or risks on natural hydrologic systems and attributing these impacts to specific water abstraction for mining, there are key considerations to be made. Recent work shows that freshwater abstraction poses the greatest risk to these desert wetland environments because freshwater abstraction has a more direct and proportionately larger impact than brine pumping<sup>42</sup>. Though the abstraction of brine water from these basins certainly carries risks of environmental impacts, no studies have shown an unambiguous or independently verifiable correlation between the abstraction of brine and critical wetlands in these basins<sup>34</sup>. In addition, reliable attribution of impacts in specific basins can only be made within an appropriate hydrological context of natural (and anthropogenic) driven climate variations, such as droughts, which have major effects on the extent and health of wetlands<sup>34</sup>.

The terms “available freshwater” and “availability minus demand” in this study are not defined as the quantity of freshwater that humans can consume without impact. Any freshwater removed from these water-scarce basins may have downgradient impacts on discharge to wetlands. We use these terms for consistency within the AWARE methodology. We do not attempt to provide specific allowable freshwater use rates, as this would require further basin-specific analysis. To improve the sustainability of lithium mining, continued research is required to quantify how lithium-related water use (freshwater and brine) will impact hydrologic systems. One possible method of addressing this challenge in the Dry Andes would be to collaborate with developers of global hydrologic models to improve the accuracy of simulated freshwater inflows for the region. Then, current or predicted freshwater consumption from mining could be added to the associated water use model. In addition, future work should focus on identifying clear relationships between brine pumping, shallow and deep freshwater resources, and sensitive wetland ecosystems. For example, brine pumping near the freshwater-brine interface could lead to interface migration due to reductions in brine hydraulic head and fluid density<sup>42</sup> or increases in lateral freshwater subsurface inflow into the brine aquifer due to a cone of depression<sup>70</sup>.

Freshwater allocations must be considered at a basin-to-sub-basin scale. In the past, freshwater has not been properly allocated within the largest lithium brine-producing basins in the world<sup>34</sup>. Variations in freshwater consumption associated with lithium processing technologies (evaporative concentration and DLE) and production targets impact water use, and these factors must be a priority when evaluating the water sustainability of a lithium brine project. For example, the only production-scale DLE operation at the Salar del Hombre Muerto consumes double the freshwater (per tonne lithium carbonate produced) than the average consumption from the evaporative concentration used at the Salar de Atacama and the Salar de Olaroz<sup>4</sup>. Estimated annual lithium production targets for advanced-stage projects in Argentina vary from 5 to 50 thousand tonnes of lithium carbonate equivalent, with a median of 25 thousand tonnes, leading to differences in expected freshwater requirements<sup>13</sup>. Because lithium mining is a reality in the Lithium Triangle, scientists, local communities, regulators, and producers must collaborate to reduce water use and monitor precipitation, streamflow, and groundwater levels to improve the understanding of each water system while maintaining the health and future existence of ecosystems.

## Methods

### Defining basins

We delineated the 28 active or prospective lithium-producing topographic watersheds using the HydroSheds product<sup>71</sup> (Fig. 4). To meet the requirements of a lithium-producing basin, each basin needed to have a clearly defined basin floor with a salar nucleus (25 basins) or saline lake (three

basins). We defined active or near-production as currently producing lithium products (lithium hydroxide, lithium carbonate, lithium chloride) or 1–3 years until full-scale production. Basin floor elevations are from the ALOS World 3D DEM.

### Precipitation assessment

Following research assessing the large and diverse array of global precipitation products available<sup>72,73</sup>, we chose a subset of products to analyze which cover gauge-based, satellite-related, and precipitation reanalysis methods. Due to specific strengths, weaknesses, and biases inherent in each of these methods, the resulting precipitation estimates for any given site can vary widely. We believe this group of datasets provides a robust assessment of the variability and diversity in precipitation available with which to determine a suitable precipitation dataset. Our approach is unique as we use Argentinian meteorological stations which largely stopped recording data in the 1990s<sup>74</sup> (green triangles within Argentina, Fig. 4). These stations are not used for calibration in global products although they provide valuable comparison points within the Lithium Triangle. While it is common for studies to assess precipitation products at monthly intervals, we chose to assess precipitation with long-term averages (11- and 21-year intervals) because the goal of the assessment was to have the most accurate input precipitation datasets for long-term average AW. The analysis presented here should not be used to inform monthly or annual precipitation product accuracy.

Meteorological precipitation data were collected from the National Meteorological and Hydrological Service of Bolivia (Senamhi), the Center for Climate and Resilience Research Climate Explorer, and the National Agricultural Technology Institute of Argentina (INTA) (see “Data availability”). Because the dates of record vary among the meteorological stations, two periods of average annual precipitation from 1980 to 1990 (19 sites) and 1996 to 2016 (seven sites) were selected to maximize the spatial and temporal distribution of observation sites. Nineteen stations have >95% complete records, while the other seven have >73% record. We compared station data with 13 global precipitation datasets<sup>62,68,75–85</sup>. For nine of the precipitation products, we calculated the average annual precipitation from both 1980–1990 and 1996–2016 for all 26 stations. For PERSIANN-CDR, average annual precipitation was calculated from 1983 to 1990 and 1996 to 2016 because the record only extends back to 1983. Only the 1996–2016 stations (seven sites) were used for GPM IMERG (2001–2016), TRMM (1998–2016), and CMORPH CDR (1998–2016) because the historical records do not extend further (Supplementary Table 1). Average annual precipitation was extracted from the gridded precipitation datasets at the point location for each meteorological station for the corresponding period of record. The accuracy of the precipitation datasets was assessed using mean absolute error and root-mean-square error between the average annual precipitation of the meteorological station data and the gridded precipitation datasets. We determined that TerraClimate produces the most accurate long-term average precipitation for the region. For detailed results see Supplementary Information.

### Availability minus demand

Various midpoint water stress indicators have been developed to quantify the impact of water use in LCA<sup>86</sup>. Common indicators include withdrawal-to-availability, consumption-to-availability, and demand-to-availability (including ecological water demands)<sup>18</sup>. These indicators represent water stress relative to use rather than availability per unit area. This can be misleading in arid regions, characterizing arid basins as less water-scarce than water-abundant basins<sup>18</sup>. The Water Use in Life Cycle Assessment (WULCA) group developed the AWARE method as the consensus water scarcity midpoint method. The AWARE method quantifies the amount of water remaining in a watershed relative to the world average after demands for humans and ecosystems have been met. We chose to represent water scarcity using the AWARE method for two reasons: (1) to maintain the consensus method to comprehensibly share our results, and (2) the AWARE method better represents arid regions and includes ecological requirements which are important factors in the



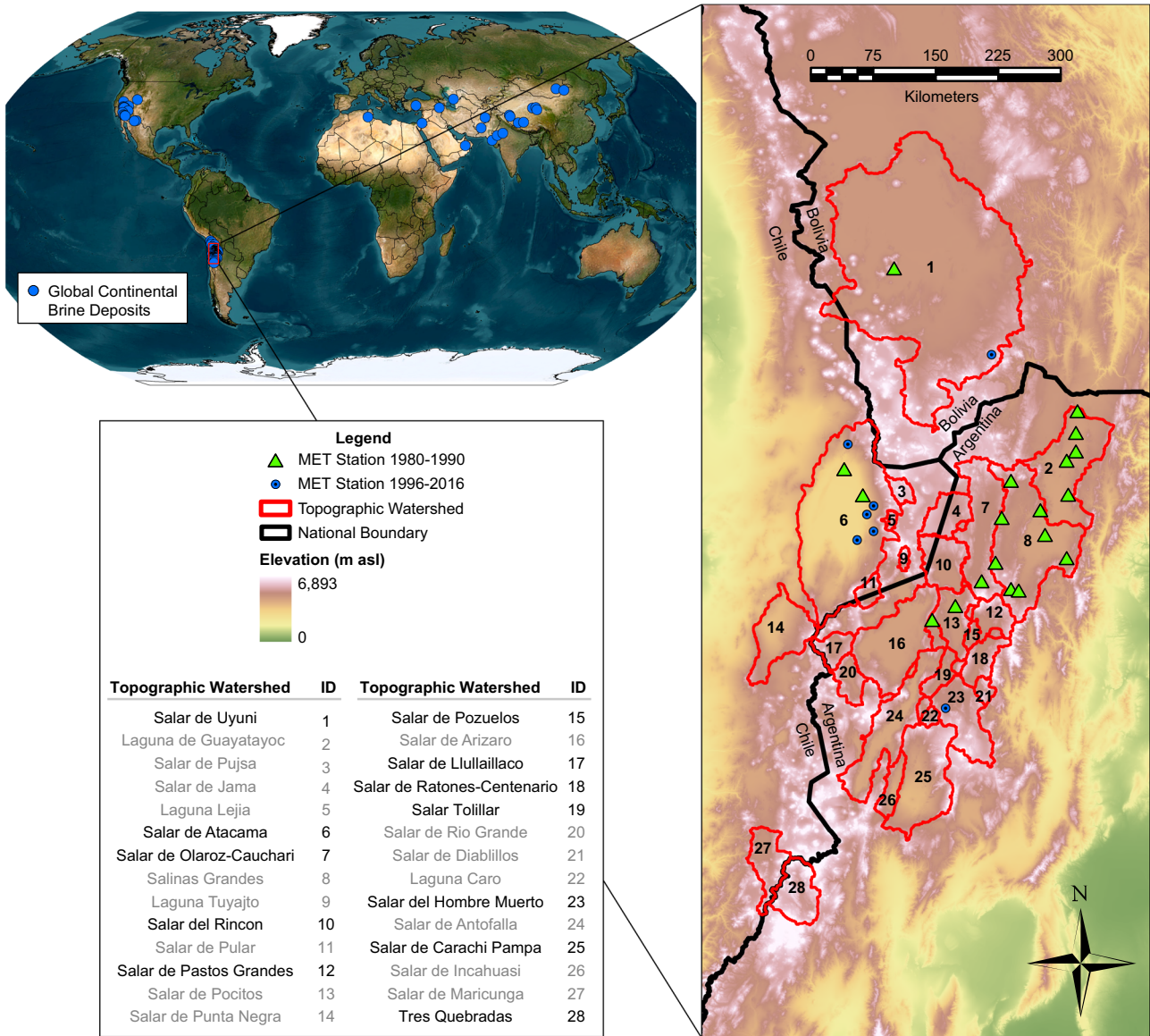


**Fig. 4 | Global distribution of continental brine deposits and map of the basins in this study.** World map showing the spatial distribution of global lithium continental brine deposits from Munk et al.<sup>10</sup> (image source: ESRI). The study region in the inset map shows topographic watersheds in red and national boundaries with black lines. Basin names and IDs are included in the lower left table with black text representing

active or near-production lithium operations and gray text representing a prospective site. The shaded background represents elevation in meters above sea level from the ALOS World 3D DEM (source: ALOS). The meteorological stations used to assess precipitation in the region are shown as green triangles or blue dots depending on their period of record.

Dry Andes. The available water and consumption datasets from WaterGAP used as input into AWARE are calculated for the year 2010 and do not include freshwater use for lithium mining. Global hydrologic models, including WaterGAP, often overestimate available water (river discharge) in arid regions like the Lithium Triangle<sup>25-27</sup>, so we recalculate AW. We do not attempt to recalculate HWC from WaterGAP because consumption (excluding mining) is minor and only accounts for 5% of freshwater demand, on average.

We modified the AWARE method from Boulay et al.<sup>18</sup> to define availability minus demand, or AMD. Table 1 provides an overview of the methodology. AMD was calculated using values of AW, HWC, and EWR:

$$AMD(mm\ year^{-1}) = \frac{AW - HWC - EWR}{Watershed\ Area} \quad (1)$$

We developed an approach to calculating AW where AW equals fresh GWR plus streamflow (R):

$$AW(mm^3\ year^{-1}) = GWR + R \quad (2)$$

We provided a range of GWR estimates by integrating three methods: (1) Extracting mean annual recharge rates (1968–2018) from Berghuijs et al.<sup>87</sup> within each basin polygon and multiplying by watershed area; (2) multiplying TerraClimate mean annual precipitation (1968–2018) by recharge fractions from Berghuijs et al.<sup>87</sup>, extracting within each basin polygon, and multiplying by watershed area; and (3) using a GWR power law function derived from the Salar de Atacama, where  $P_{RCH\ Zone}$  is TerraClimate mean annual precipitation in  $mm\ year^{-1}$  within the recharge zone and  $Area_{RCH\ Zone}$  is the area of the recharge zone in  $mm^2$ <sup>30</sup>. The recharge zone is defined as the watershed

**Table 1 | Summary table of calculation methods and references used for the Lithium Closed Basin Water Availability Model**

Water availability component	Calculation	Method reference
Fresh groundwater recharge (GWR)	1. Boultt et al. <sup>30</sup> GWR fraction × TerraClimate Pr 2. Berghuijs et al. <sup>87</sup> GWR fraction × TerraClimate Pr 3. Berghuijs et al. <sup>87</sup> GWR	Kirshen et al. (This Study); Berghuijs et al. <sup>87</sup>
Streamflow (R)	Calibrated streamflow coefficient range (0.07–0.16) × TerraClimate Pr	Kirshen et al. (This Study)
Available freshwater (AW)	Fresh groundwater recharge + streamflow	Kirshen et al. (This Study)
Environmental water requirements (EWR)	0.45 × available freshwater	Pastor et al. <sup>89</sup> ; Boulay et al. <sup>18</sup>
Human water consumption (HWC)	Extracted from WaterGAP model	Flörke et al. <sup>88</sup> ; Müller Schmied et al. <sup>63</sup>
Freshwater demand	Environmental water requirements + human water consumption	Boulay et al. <sup>18</sup>
Availability minus demand (AMD)	Available freshwater – freshwater demand	Boulay et al. <sup>18</sup>

area minus the basin floor area (see Supplementary Table 3).

$$GWR_{method3} (mm^3 year^{-1}) = (1.3 \times 10^{-4}) \times P_{RCHZone}^{2.3} \times Area_{RCHZone} \quad (3)$$

For GWR methods 2 and 3, the TerraClimate datasets were modified with the Pixel Editor Imagery tool in ArcGIS Pro within basins 13, 16, 23, and 25 because the white salar nucleus was interpreted as cloud coverage, so precipitation was overestimated on the basin floor.

Streamflow was calculated using the following equations, where *C* is the streamflow coefficient,  $P_{RCH\ Zone}$  is TerraClimate precipitation in mm year<sup>-1</sup> within the recharge zone, and  $Area_{RCH\ Zone}$  is the area of the recharge zone in mm<sup>2</sup>.

$$R (mm^3 year^{-1}) = (C \times P_{RCHZone} \times Area_{RCHZone}) \quad (4)$$

The streamflow coefficient (*C*) is shown in the following equation, where  $R_{RCH\ Zone}$  is basin-wide streamflow (mm<sup>3</sup> year<sup>-1</sup>) from field measurements in three basins—Salar de Atacama, Salar de Pastos Grandes, and Salar del Hombre Muerto.

$$C = \left( \frac{R_{RCHZone}}{Area_{RCHZone}} \right) / P_{RCHZone} \quad (5)$$

These measurements were collected during several field campaigns between 2019 and 2023 using an OTT MF pro-Water Flow Meter and a USGS TopSet Wading Rod. These data were supplemented where necessary with measurements collected by the Dirección General de Aguas and environmental consultants to lithium mines. These three basins represent a relatively wide range of elevations and geographic coverage. Streamflow was calculated using the recharge zone because the vast majority of streamflow in these systems exists outside the basin floor. We use the average (0.11), minimum (0.07), and maximum (0.16) of *C* from the three basins to define streamflow bounds. The lower bound of AW was calculated as minimum GWR plus minimum *R*, and the upper bound of AW was calculated as maximum GWR plus maximum *R*. Average AW was calculated as the average of the three GWR methods plus average *R*. The average and upper and lower bounds of AMD were calculated using the AW values discussed in the previous sentence.

We used methods from Boulay et al.<sup>18</sup> to quantify HWC and EWR. HWC from WaterGAP<sup>63,88</sup> was downloaded from the WULCA AWARE website (see Data Availability). First, the data were normalized by grid area and resampled from 0.5° resolution to 0.02° resolution. Then the average consumption was extracted within each basin polygon and multiplied by the area of the basin polygon. EWR were calculated as 0.45 multiplied by the average AW. We assumed intermediate flow because we used annual averages of streamflow<sup>18,89</sup>. We included GWR as part of the EWR calculation because groundwater plays a key role in supporting wetlands and ecosystems in these environments.

### Comparison with WaterGAP 2.2 and PCR-GLOBWB 2.0

We extracted the mean annual simulated river discharge from the WaterGAP (1960–2010) and PCR-GLOBWB (1958–2015) to compare with measured streamflow and results from this study. Actual mean monthly river availability data from WaterGAP was from the WULCA AWARE website and PCR-GLOBWB data was extracted from the Utrecht University Yoda data portal (see Data Availability). Both datasets were normalized by grid area and resampled to 0.02° before extracting the mean annual discharge from each basin polygon. Extracted values were then multiplied by the basin area. In addition, we extracted monthly precipitation from the Utrecht University Yoda data portal to calculate the percent of precipitation that becomes streamflow.

CFs were calculated using the following equation<sup>18</sup>. The CFs for Fig. 3 were calculated using mean AMD. A range of CF values were calculated based on the upper and lower bounds of AW (Supplementary Table 2).  $AMD_{world\ avg}$  is 163 mm year<sup>-1</sup> (or 0.0136 m month<sup>-1</sup>):

$$CF = \frac{1}{\left( \frac{AMD}{AMD_{world\ avg}} \right)} \quad (6)$$

For WaterGAP and PCR-GLOBWB, we defined AW as river discharge. This was a conservative approach to define an upper bound on the CF. If GWR was included, CF values would decrease, and these products would further underestimate water scarcity. EWR was the product of 0.45 and river discharge, and HWC values are the same used in this study for consistency. Water scarcity was classified for each basin using CF cutoff values from Schomberg et al.<sup>48</sup>.

Boulay et al.<sup>18</sup> calculated AMD and CF at monthly time steps, while our approach (LiCBWA) was calculated using long-term averages. If we calculated AMD at monthly time steps, differences could arise in CF and EWR values; the original AWARE method calculated EWR based on low, intermediate, and high flows. We assumed that average annual flows are intermediate. These factors do not influence the findings from the study because we re-calculated AMD and CF for WaterGAP and PCR-GLOBWB using long-term averages of streamflow. In addition, these arid closed-basin systems have relatively inconsistent monthly climate and freshwater inflow patterns, so monthly CF calculations could be less accurate and less representative than the long-term averages.

We also re-calculated CF from WaterGAP instead of extracting values from already calculated CF from Boulay et al.<sup>18</sup> because Boulay et al.<sup>18</sup> had gaps in spatial coverage in the study region; when extracting CF values directly from Boulay et al.<sup>18</sup>, nine basins are considered critical, seven are semi-critical, three are uncritical, and nine have more than half of basin area with no data.

### Data availability

Meteorological station data was extracted from the following locations: National Meteorological and Hydrological Service of Bolivia (<http://>



senamhi.gob.bo/index.php/onsc), Center for Climate and Resilience Research Climate Explorer (<https://explorador.cr2.cl/>), and the National Agricultural Technology Institute of Argentina (INTA; Bianchi et al.,<sup>74</sup>). Precipitation data were downloaded from the following locations: TerraClimate ([https://developers.google.com/earth-engine/datasets/catalog/IDAHO\\_EPSCOR\\_TERRACLIMATE](https://developers.google.com/earth-engine/datasets/catalog/IDAHO_EPSCOR_TERRACLIMATE)), WFDEI (<ftp://rfddata:forceDATA@ftp.iiasa.ac.at>), CRU TS 4.07 (<https://crudata.uea.ac.uk/cru/data/hrg/>), GPCP, GPCC, CHIRPS (<https://climatedataguide.ucar.edu/climate-data/gpcp-global-precipitation-climatology-centre>), PERSIANN-CDR (<https://chrsdata.eng.uci.edu/>), MSWEP V2.2 (<https://www.gloh2o.org/mswep/>), ERA-5 (<https://cds.climate.copernicus.eu/cdsapp#!/search?type=dataset>), CMORPH CDR (<https://www.ncei.noaa.gov/data/cmorph-high-resolution-global-precipitation-estimates/access/daily/0.25deg/>), GPM IMERG L3 V06 (<https://search.earthdata.nasa.gov/search>), TRMM 3B43 V7, CFSV2. Groundwater recharge and groundwater recharge fractions from Berghuijs et al.<sup>87</sup> were downloaded from (<https://zenodo.org/records/7611675>). Human water consumption (“TOT\_CU”) and river discharge from WaterGAP 2.2 were downloaded from (<https://wulca-waterlca.org/aware/input-data-watergap/>), and river discharge (“discharge\_monthAvg”) and precipitation (“precipitation\_monthTot”) from PCR-GLOBWB 2.0 was from ([https://github.com/UU-Hydro/PCR-GLOBWB\\_model](https://github.com/UU-Hydro/PCR-GLOBWB_model)). Basin attributes, model output, and data for the precipitation assessment can be found in this online data repository (<https://doi.org/10.6084/m9.figshare.25505149>).

Received: 5 April 2024; Accepted: 13 February 2025;

Published online: 26 March 2025

## References

- Lee, H. et al. *Climate Change 2023: Synthesis Report. Contribution of Working Groups I, II and III to the Sixth Assessment Report of the Intergovernmental Panel on Climate Change* (The Australian National University, 2023).
- Trahey, L. et al. Energy storage emerging: a perspective from the Joint Center for Energy Storage Research. *Proc. Natl. Acad. Sci. USA* **117**, 12550–12557 (2020).
- Haddad, A. Z. et al. How to make lithium extraction cleaner, faster and cheaper—in six steps. *Nature* **616**, 245–248 (2023).
- Vera, M. L., Torres, W. R., Galli, C. I., Chagnes, A. & Flexer, V. Environmental impact of direct lithium extraction from brines. *Nat. Rev. Earth Environ.* **4**, 149–165 (2023).
- U.S. Geological Survey. *Mineral Commodity Summaries 2023*. <https://doi.org/10.3133/mcs2023> (U.S. Geological Survey, 2023).
- Munk, L. A., Boutt, D. F., Hynek, S. A. & Moran, B. J. Hydrogeochemical fluxes and processes contributing to the formation of lithium-enriched brines in a hyper-arid continental basin. *Chem. Geol.* **493**, 37–57 (2018).
- Corenthal, L. G., Boutt, D. F., Hynek, S. A. & Munk, L. A. Regional groundwater flow and accumulation of a massive evaporite deposit at the margin of the Chilean Altiplano. *Geophys. Res. Lett.* **43**, 8017–8025 (2016).
- Eugster, H. P. Geochemistry of evaporitic lacustrine deposits. *Annu. Rev. Earth Planet. Sci.* **8**, 35 (1980).
- Rosen, M. R. The importance of groundwater in playas: a review of playa classifications and the sedimentology and hydrology of playas. In *Paleoclimate and Basin Evolution of Playa Systems* Vol. 289 (ed. Rosen, M. R.) (Geological Society of America, 1994).
- Munk, L. A. et al. Lithium brines: origin, characteristics, and global distribution. *Rev. Econ. Geol.* (2025).
- Munk, L. A. et al. Lithium brines: a global perspective. *Rev. Econ. Geol.* **18**, 339–365 (2016).
- Khalil, A., Mohammed, S., Hashaikeh, R. & Hilal, N. Lithium recovery from brine: recent developments and challenges. *Desalination* **528**, 115611 (2022).
- Ministerio de Economía Argentina. *Portfolio of Advanced Projects Lithium*. <https://www.argentina.gob.ar/portofolio-mining-projects-2024> (Ministerio de Economía Argentina, 2024).
- Marconi, P., Arengo, F. & Clark, A. The arid Andean plateau waterscapes and the lithium triangle: flamingos as flagships for conservation of high-altitude wetlands under pressure from mining development. *Wetl. Ecol. Manag.* **30**, 827–852 (2022).
- Houston, J. A recharge model for high altitude, arid, Andean aquifers. *Hydrol. Process. Int. J.* **23**, 2383–2393 (2009).
- Bookhagen, B. & Strecker, M. R. Orographic barriers, high-resolution TRMM rainfall, and relief variations along the eastern Andes. *Geophys. Res. Lett.* **35**, L06403 (2008).
- Strecker, M. R. et al. Tectonics and climate of the southern central Andes. *Annu. Rev. Earth Planet. Sci.* **35**, 747–787 (2007).
- Boulay, A.-M. et al. The WULCA consensus characterization model for water scarcity footprints: assessing impacts of water consumption based on Available Water Remaining (AWARE). *Int J. Life Cycle Assess.* **23**, 368–378 (2018).
- Bierkens, M., Wanders, N., Droppers, B. & Leijnse, M. National Geographic Society World Water Map. [worldwatermap.nationalgeographic.org](http://worldwatermap.nationalgeographic.org) (2023).
- Kuzma, S. et al. *Aqueduct 4.0: Updated Decision-Relevant Global Water Risk Indicators* (World Resources Institute, 2023).
- WWF. Water Risk Filter. [riskfilter.org/water/explore/map](http://riskfilter.org/water/explore/map) (2021).
- Bierkens, M. F. P. Global hydrology 2015: State, trends, and directions. *Water Resour. Res.* **51**, 4923–4947 (2015).
- Sood, A. & Smakhtin, V. Global hydrological models: a review. *Hydrol. Sci. J.* **60**, 549–565 (2015).
- Wada, Y. et al. Human–water interface in hydrological modelling: current status and future directions. *Hydrol. Earth Syst. Sci.* **21**, 4169–4193 (2017).
- Gnann, S. et al. Functional relationships reveal differences in the water cycle representation of global water models. *Nat. Water* **1**, 1079–1090 (2023).
- Haddeland, I. et al. Multimodel estimate of the global terrestrial water balance: setup and first results. *J. Hydrometeorol.* **12**, 869–884 (2011).
- Trambauer, P., Maskey, S., Winsemius, H., Werner, M. & Uhlenbrook, S. A review of continental scale hydrological models and their suitability for drought forecasting in (sub-Saharan) Africa. *Phys. Chem. Earth Parts A B C.* **66**, 16–26 (2013).
- Telciu, C.-E. et al. Understanding each other’s models: an introduction and a standard representation of 16 global water models to support intercomparison, improvement, and communication. *Geosci. Model Dev.* **14**, 3843–3878 (2021).
- Houston, J. Recharge to groundwater in the Turi Basin, northern Chile: an evaluation based on tritium and chloride mass balance techniques. *J. Hydrol.* **334**, 534–544 (2007).
- Boutt, D. F., Corenthal, L. G., Moran, B. J., Munk, L. & Hynek, S. A. Imbalance in the modern hydrologic budget of topographic catchments along the western slope of the Andes (21–25 S): implications for groundwater recharge assessment. *Hydrogeol. J.* **29**, 985–1007 (2021).
- Tyler, S. W., Muñoz, J. F. & Wood, W. W. The response of playa and sabkha hydraulics and mineralogy to climate forcing. *Groundwater* **44**, 329–338 (2006).
- McKnight, S. V., Boutt, D. F. & Munk, L. A. Impact of hydrostratigraphic continuity on brine-to-freshwater interface dynamics: implications from a two-dimensional parametric study in an arid and endorheic basin. *Water Resour. Res.* **57**, e2020WR028302 (2021).
- Moran, B. J., Boutt, D. F., Munk, L. A. & Fisher, J. D. Contemporary and relic waters strongly decoupled in arid alpine environments. *PLOS Water* **3**, e0000191 (2024).
- Moran, B. J. et al. Relic groundwater and prolonged drought confound interpretations of water sustainability and lithium extraction in arid lands. *Earths Future* **10**, e2021EF002555 (2022).

35. de la Fuente, A., Meruane, C. & Suárez, F. Long-term spatiotemporal variability in high Andean wetlands in northern Chile. *Sci. Total Environ.* **756**, 143830 (2021).
36. Frau, D. et al. Hydroclimatological patterns and limnological characteristics of unique wetland systems on the Argentine high Andean Plateau. *Hydrology* **8**, 164 (2021).
37. Farias, M. E. et al. Prokaryotic diversity and biogeochemical characteristics of benthic microbial ecosystems at La Brava, a hypersaline lake at Salar de Atacama, Chile. *PLoS ONE* **12**, e0186867 (2017).
38. Scanlon, B. R., Healy, R. W. & Cook, P. G. Choosing appropriate techniques for quantifying groundwater recharge. *Hydrogeol. J.* **10**, 18–39 (2002).
39. Moran, B. J., Boutt, D. F. & Munk, L. A. Stable and radioisotope systematics reveal fossil water as fundamental characteristic of arid orogenic-scale groundwater systems. *Water Resour. Res.* **55**, 11295–11315 (2019).
40. McKnight, S. V., Boutt, D. F., Munk, L. A. & Moran, B. Distinct hydrologic pathways regulate perennial surface water dynamics in a hyperarid basin. *Water Resour. Res.* **59**, e2022WR034046 (2023).
41. Marazueta, M. A 3D mapping, hydrodynamics and modelling of the freshwater-brine mixing zone in salt flats similar to the Salar de Atacama (Chile). *J. Hydrol.* **561**, 223–235 (2018).
42. Corkran, D. B. et al. Density Constrains Environmental Impacts of Fluid Abstraction in Continental Lithium Brines. *ESS Open Arch.* <https://doi.org/10.22541/essoar.173325192.22768610/v1> (2024).
43. Babidge, S., Kalazich, F., Prieto, M. & Yager, K. That's the problem with that lake; it changes sides': mapping extraction and ecological exhaustion in the Atacama. *J. Polit. Ecol.* **26**, 738–760 (2019).
44. Marazueta, M. A., Vázquez-Suñé, E., Ayora, C. & García-Gil, A. Towards more sustainable brine extraction in salt flats: learning from the Salar de Atacama. *Sci. Total Environ.* **703**, 135605 (2020).
45. Kelly, J. C., Wang, M., Dai, Q. & Winjobi, O. Energy, greenhouse gas, and water life cycle analysis of lithium carbonate and lithium hydroxide monohydrate from brine and ore resources and their use in lithium ion battery cathodes and lithium ion batteries. *Resour. Conserv. Recycl.* **174**, 105762 (2021).
46. Pell, R. et al. Towards sustainable extraction of technology materials through integrated approaches. *Nat. Rev. Earth Environ.* **2**, 665–679 (2021).
47. Schenker, V., Oberschelp, C. & Pfister, S. Regionalized life cycle assessment of present and future lithium production for Li-ion batteries. *Resour. Conserv. Recycl.* **187**, 106611 (2022).
48. Schomberg, A. C., Bringezu, S. & Flörke, M. Extended life cycle assessment reveals the spatially-explicit water scarcity footprint of a lithium-ion battery storage. *Commun. Earth Environ.* **2**, 11 (2021).
49. Schomberg, A. C. & Bringezu, S. How can the water use of lithium brine mining be adequately assessed? *Resour. Conserv. Recycl.* **190**, 106806 (2023).
50. Stamp, A., Lang, D. J. & Wäger, P. A. Environmental impacts of a transition toward e-mobility: the present and future role of lithium carbonate production. *J. Clean. Prod.* **23**, 104–112 (2012).
51. Liu, W. & Agusdinata, D. B. Interdependencies of lithium mining and communities sustainability in Salar de Atacama, Chile. *J. Clean. Prod.* **260**, 120838 (2020).
52. Liu, W., Agusdinata, D. B. & Myint, S. W. Spatiotemporal patterns of lithium mining and environmental degradation in the Atacama Salt Flat, Chile. *Int. J. Appl. Earth Observation Geoinf.* **80**, 145–156 (2019).
53. Flexer, V., Baspineiro, C. F. & Galli, C. I. Lithium recovery from brines: a vital raw material for green energies with a potential environmental impact in its mining and processing. *Sci. Total Environ.* **639**, 1188–1204 (2018).
54. Gajardo, G., Redón, S. Andean hypersaline lakes in the Atacama Desert, northern Chile: between lithium exploitation and unique biodiversity conservation. *Conserv. Sci. Pr.* **1**, e94 (2019).
55. Gutiérrez, J. S. et al. Climate change and lithium mining influence flamingo abundance in the Lithium Triangle. *Proc. R. Soc. B* **289**, 20212388 (2022).
56. Agusdinata, D. B., Liu, W., Eakin, H. & Romero, H. Socio-environmental impacts of lithium mineral extraction: towards a research agenda. *Environ. Res. Lett.* **13**, 123001 (2018).
57. Rodell, M. et al. Emerging trends in global freshwater availability. *Nature* **557**, 651–659 (2018).
58. Chordia, M., Wickerts, S., Nordelöf, A. & Arvidsson, R. Life cycle environmental impacts of current and future battery-grade lithium supply from brine and spodumene. *Resour. Conserv. Recycl.* **187**, 106634 (2022).
59. Halkes, R. T. et al. Life cycle assessment and water use impacts of lithium production from salar deposits: challenges and opportunities. *Resour. Conserv. Recycl.* **207**, 107554 (2024).
60. Marinova, S., Roche, L., Link, A. & Finkbeiner, M. Water footprint of battery-grade lithium production in the Salar de Atacama, Chile. *J. Clean. Prod.* **487**, 144635 (2025).
61. Blin, N., Hausner, M., Leray, S., Lowry, C. & Suárez, F. Potential impacts of climate change on an aquifer in the arid Altiplano, northern Chile: the case of the protected wetlands of the Salar del Huasco basin. *J. Hydrol. Reg. Stud.* **39**, 100996 (2022).
62. Abatzoglou, J. T., Dobrowski, S. Z., Parks, S. A. & Hegewisch, K. C. TerraClimate, a high-resolution global dataset of monthly climate and climatic water balance from 1958–2015. *Sci. Data* **5**, 1–12 (2018).
63. Müller Schmied, H. et al. Sensitivity of simulated global-scale freshwater fluxes and storages to input data, hydrological model structure, human water use and calibration. *Hydrol. Earth Syst. Sci.* **18**, 3511–3538 (2014).
64. Sutanudjaja, E. H. et al. PCR-GLOBWB 2: a 5 arcmin global hydrological and water resources model. *Geosci. Model Dev.* **11**, 2429–2453 (2018).
65. Gain, A. K., Giupponi, C. & Wada, Y. Measuring global water security towards sustainable development goals. *Environ. Res. Lett.* **11**, 124015 (2016).
66. Schewe, J. et al. Multimodel assessment of water scarcity under climate change. *Proc. Natl. Acad. Sci. USA* **111**, 3245–3250 (2014).
67. Kampf, S. K. & Tyler, S. W. Spatial characterization of land surface energy fluxes and uncertainty estimation at the Salar de Atacama, Northern Chile. *Adv. Water Resour.* **29**, 336–354 (2006).
68. Weedon, G. P. et al. The WFDEI meteorological forcing data set: WATCH Forcing Data methodology applied to ERA-Interim reanalysis data. *Water Resour. Res.* **50**, 7505–7514 (2014).
69. Liu, Y., Wagener, T., Beck, H. E. & Hartmann, A. What is the hydrologically effective area of a catchment? *Environ. Res. Lett.* **15**, 104024 (2020).
70. Houston, J., Butcher, A., Ehren, P., Evans, K. & Godfrey, L. The evaluation of brine prospects and the requirement for modifications to filing standards. *Econ. Geol.* **106**, 1225–1239 (2011).
71. Lehner, B., Verdin, K. & Jarvis, A. New global hydrography derived from spaceborne elevation data. *Eos Trans. Am. Geophys. Union* **89**, 93–94 (2008).
72. Dubey, S., Gupta, H., Goyal, M. K. & Joshi, N. Evaluation of precipitation datasets available on Google Earth engine over India. *Int. J. Climatol.* **41**, 4844–4863 (2021).
73. Sun, Q. et al. A review of global precipitation data sets: Data sources, estimation, and intercomparisons. *Rev. Geophys.* **56**, 79–107 (2018).

74. Bianchi, A. R., Yañez, C. E. & Acuña, L. R. *Base de Datos Mensuales de Precipitaciones del Noroeste Argentino. Informe del Proyecto Riesgo Agropecuario* (INTA-SAGPYA, 2005).
75. Schneider, U. et al. GPCC's new land surface precipitation climatology based on quality-controlled in situ data and its role in quantifying the global water cycle. *Theor. Appl. Climatol.* **115**, 15–40 (2014).
76. Funk, C. et al. The climate hazards infrared precipitation with stations – a new environmental record for monitoring extremes. *Sci. Data* **2**, 1–21 (2015).
77. Adler, R. F. et al. The Global Precipitation Climatology Project (GPCP) monthly analysis (new version 2.3) and a review of 2017 global precipitation. *Atmosphere* **9**, 138 (2018).
78. Saha, S. et al. The NCEP climate forecast system version 2. *J. Clim.* **27**, 2185–2208 (2014).
79. Beck, H. E. et al. MSWEP V2 global 3-hourly 0.1 precipitation: methodology and quantitative assessment. *Bull. Am. Meteorol. Soc.* **100**, 473–500 (2019).
80. Hersbach, H. et al. The ERA5 global reanalysis. *Q. J. R. Meteorol. Soc.* **146**, 1999–2049 (2020).
81. Ashouri, H. et al. PERSIANN-CDR: Daily precipitation climate data record from multisatellite observations for hydrological and climate studies. *Bull. Am. Meteorol. Soc.* **96**, 69–83 (2015).
82. Huffman, G.J. et al. NASA global precipitation measurement (GPM) integrated multi satellite retrievals for GPM (IMERG). Algorithm theoretical basis document (ATBD) version 4, 2020–2025 (2015).
83. Huffman, G. J. et al. The TRMM multisatellite precipitation analysis (TMPA): Quasi-global, multiyear, combined-sensor precipitation estimates at fine scales. *J. Hydrometeorol.* **8**, 38–55 (2007).
84. Xie, P. et al. Reprocessed, bias-corrected CMORPH global high-resolution precipitation estimates from 1998. *J. Hydrometeorol.* **18**, 1617–1641 (2017).
85. Harris, I., Osborn, T. J., Jones, P. & Lister, D. Version 4 of the CRU TS monthly high-resolution gridded multivariate climate dataset. *Sci. Data* **7**, 109 (2020).
86. Boulay, A.-M. et al. Consensus building on the development of a stress-based indicator for LCA-based impact assessment of water consumption: outcome of the expert workshops. *Int. J. Life Cycle Assess.* **20**, 577–583 (2015).
87. Berghuijs, W. R., Luijendijk, E., Moeck, C., van der Velde, Y. & Allen, S. T. Global recharge data set indicates strengthened groundwater connection to surface fluxes. *Geophys. Res. Lett.* **49**, e2022GL099010 (2022).
88. Flörke, M. et al. Domestic and industrial water uses of the past 60 years as a mirror of socio-economic development: a global simulation study. *Glob. Environ. Change* **23**, 144–156 (2013).
89. Pastor, A. V., Ludwig, F., Biemans, H., Hoff, H. & Kabat, P. Accounting for environmental flow requirements in global water assessments. *Hydrol. Earth Syst. Sci.* **18**, 5041–5059 (2014).

## Acknowledgements

The authors would like to thank BMW Group and BASF for funding and supporting this research. We thank Dr. Nicole Blin (University of Massachusetts Amherst) for valuable feedback on the methods and during the writing process.

## Author contributions

A. Kirshen, B. Moran, and D. Boutt designed the research; A. Kirshen, A. Russo, J. Jenckes, and M. Bresee collected and processed the data; A. Kirshen analyzed the data and developed the figures; A. Kirshen drafted the manuscript; A. Kirshen, B. Moran, L.A. Munk, A. Russo, S. McKnight, J. Jenckes, D. Corkran, M. Bresee, and D. Boutt reviewed and revised the manuscript.

## Competing interests

The authors declare no competing interests.

## Additional information

**Supplementary information** The online version contains supplementary material available at <https://doi.org/10.1038/s43247-025-02130-6>.

**Correspondence** and requests for materials should be addressed to Alexander B. Kirshen.

**Peer review information** *Communications Earth and Environment* thanks Victoria Flexer, Anna Schomberg, and the other, anonymous, reviewer(s) for their contribution to the peer review of this work. Primary Handling Editors: Heike Langenberg. A peer review file is available.

**Reprints and permissions information** is available at <http://www.nature.com/reprints>

**Publisher's note** Springer Nature remains neutral with regard to jurisdictional claims in published maps and institutional affiliations.

**Open Access** This article is licensed under a Creative Commons Attribution 4.0 International License, which permits use, sharing, adaptation, distribution and reproduction in any medium or format, as long as you give appropriate credit to the original author(s) and the source, provide a link to the Creative Commons licence, and indicate if changes were made. The images or other third party material in this article are included in the article's Creative Commons licence, unless indicated otherwise in a credit line to the material. If material is not included in the article's Creative Commons licence and your intended use is not permitted by statutory regulation or exceeds the permitted use, you will need to obtain permission directly from the copyright holder. To view a copy of this licence, visit <http://creativecommons.org/licenses/by/4.0/>.

© The Author(s) 2025